Volume 61
Number 76
28 September 2025
Pages 14461–14730

ChemComm

Chemical Communications

rsc.li/chemcomm

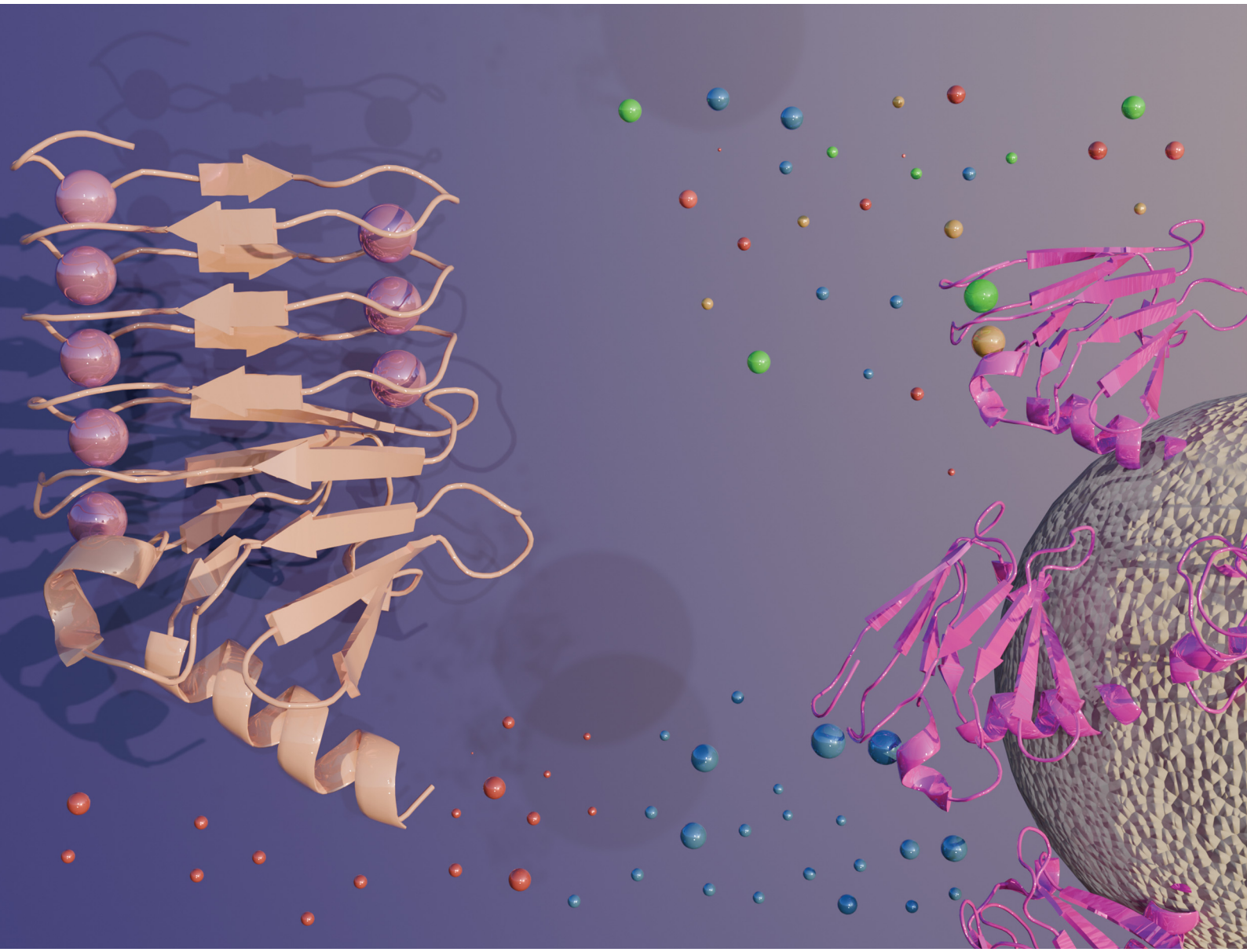

ISSN 1359-7345

ROYAL SOCIETY OF CHEMISTRY

COMMUNICATION

Scott Banta *et al.*

Reducing binding site heterogeneity *via* truncation of the RTX domain enhances selectivity for rare earth element separation

ChemComm

COMMUNICATION

View Article Online
View Journal | View Issue

Cite this: *Chem. Commun.*, 2025, **61**, 14629

Received 16th July 2025,
Accepted 9th August 2025

DOI: 10.1039/d5cc03992d

rsc.li/chemcomm

Reducing binding site heterogeneity *via* truncation of the RTX domain enhances selectivity for rare earth element separation

Farid F. Khoury, [a] Sameera Abeyarthna, [a] Bradley S. Heater,[b] Katarzyna H. Kucharzyk[b] and Scott Banta *[a]

Rare earth elements (REEs) are critical components of modern technologies but present a notoriously difficult separation challenge. Here, we report a rationally truncated variant of the calcium-binding RTX domain that improves REE selectivity by reducing binding site heterogeneity. The engineered scaffold, RTX(2), exhibits improved binding affinity, structure stability, pH-tunable elution, and enhanced chromatographic resolution, achieving over 200-fold selectivity within the REE series.

Efficient separation of REEs remains a critical bottleneck in securing sustainable access to materials that power modern technologies.[1] Despite their indispensable roles in electronics, clean energy, and defense, REEs remain notoriously difficult to purify due to their nearly indistinguishable physical and chemical properties.[1,2] Industrial processes still rely on solvent-intensive liquid–liquid extraction, which is environmentally costly and requires numerous stages to achieve desired purities.[1–3] Emerging biological strategies offer a fundamentally different approach in which natural and engineered proteins can distinguish REEs with remarkable specificity. These include lanthanide-binding tags (LBT),[4] small peptides developed through combinatorial engineering to bind lanthanides, lanmodulins (LanM),[5] naturally occurring lanthanide-binding proteins with picomolar affinities, and calcium-binding proteins,[6] which exhibit intrinsic affinity for REE due to chemical similarity with calcium ions.

Chromatography systems with immobilized proteins have made significant strides in leveraging protein selectivity to separate individual REEs. For example, LanM-based columns have demonstrated single-stage separation of non-REEs and have been used to separate mixtures of neodymium and dysprosium, two major components of NdFeB permanent magnets, with greater than 95% purity and yield.[7,8] In multi-stage systems, LanM has also enabled the individual separation of scandium and yttrium and group separation of lanthanides into light, middle, and heavy fractions through combined pH- and chelator-based elution strategies.[9] More recently, HEW5, a newly discovered high-capacity calcium-binding protein with a strong ability to discriminate between light REEs, was immobilized and used to achieve single-stage, chelator-free separation of lanthanum and neodymium with over 90% purity and yield, which are two predominant REEs in bastnäsite mining concentrates.[10] These studies demonstrate that protein-based systems can serve as a modular and sustainable platform for selective REE separation. However, improvement in the selectivity of the proteins is still necessary to fractionate complex REE mixtures into their individual components in single chromatographic steps.

Proteins often exhibit a parabolic affinity preference, favoring intermediate REEs,[8–12] unlike strong chelators such as citrate and EDTA, which show increasing binding affinities across the lanthanide series. This trend likely arises from a thermodynamic interplay between the hydration energy, charge density, and the geometric fit of the ion within the binding pocket of the protein.[13,14] That fit, in turn, is governed by the coordination geometry and the structural features of the binding site. Binding site rigidity plays a central role in this selectivity: while flexible binding environments can accommodate a broader range of ions, more rigid architectures can exclude suboptimal fits, thereby enhancing ion discrimination.[15] Beyond the first coordination shell, second-shell interactions, particularly hydrogen bond networks, can further stabilize preferred geometries and refine selectivity. This has been observed in LBTs and *Hans*-LanM.[8,16] However, many natural proteins contain multiple, structurally distinct binding sites, which can lead to heterogeneous ion preferences across a protein. This feature can broaden elution profiles in chromatographic systems. To address these challenges, we investigated the impact of site heterogeneity by rationally truncating a high-capacity calcium-binding protein to isolate its most selective

[a] *Department of Chemical Engineering, Columbia University, New York, NY 10027, USA. E-mail: sb2373@columbia.edu*
[b] *Battelle Memorial Research Institute, Columbus, OH 43201, USA*

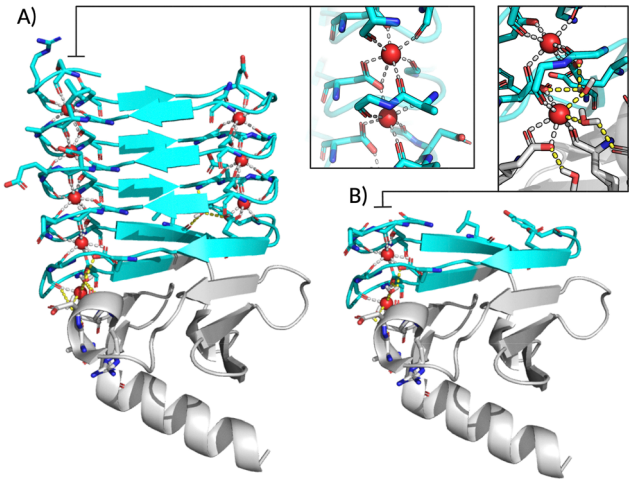

Fig. 1 (A) Crystal structure of block V of the RTX domain, RTX(8), showing eight calcium-bound sites (PDB ID: 5CVW). (B) Truncated scaffold RTX(2), retaining the two C-terminal calcium-binding sites. Inset: Calcium coordination geometries vary across RTX(8), with the RTX(2) region exhibiting a dense, water-mediated second-shell hydrogen-bonding network. Gray dashed lines represent coordination bonds to protein residues, and yellow dashed lines indicate water-mediated coordination and hydrogen bonding interactions.

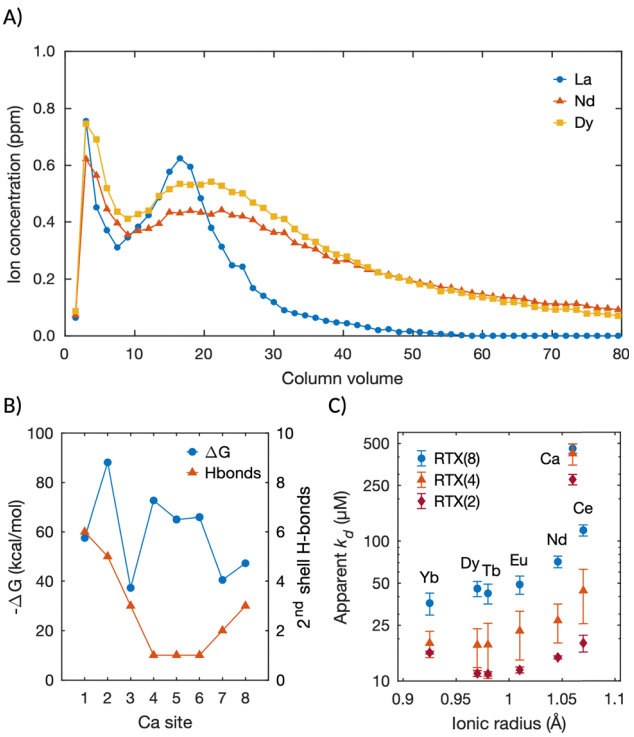

Fig. 2 (A) Isocratic elution profile of a La/Nd/Dy mixture using RTX(8), showing overlapping peaks and low separation resolution at pH 5.0. (B) Analysis of binding free energy (Δ*G*) for calcium in RTX(8), highlighting stronger affinities at the C-terminal sites, and second-shell hydrogen-bond networks, with RTX(2) sites exhibiting dense water-mediated stabilization. (C) Apparent dissociation constants (K_d) for REEs measured by FRET-based titrations of RTX(8), RTX(4), and RTX(2), showing increased binding affinity upon truncation. Error bars represent 95% confidence intervals of fits.

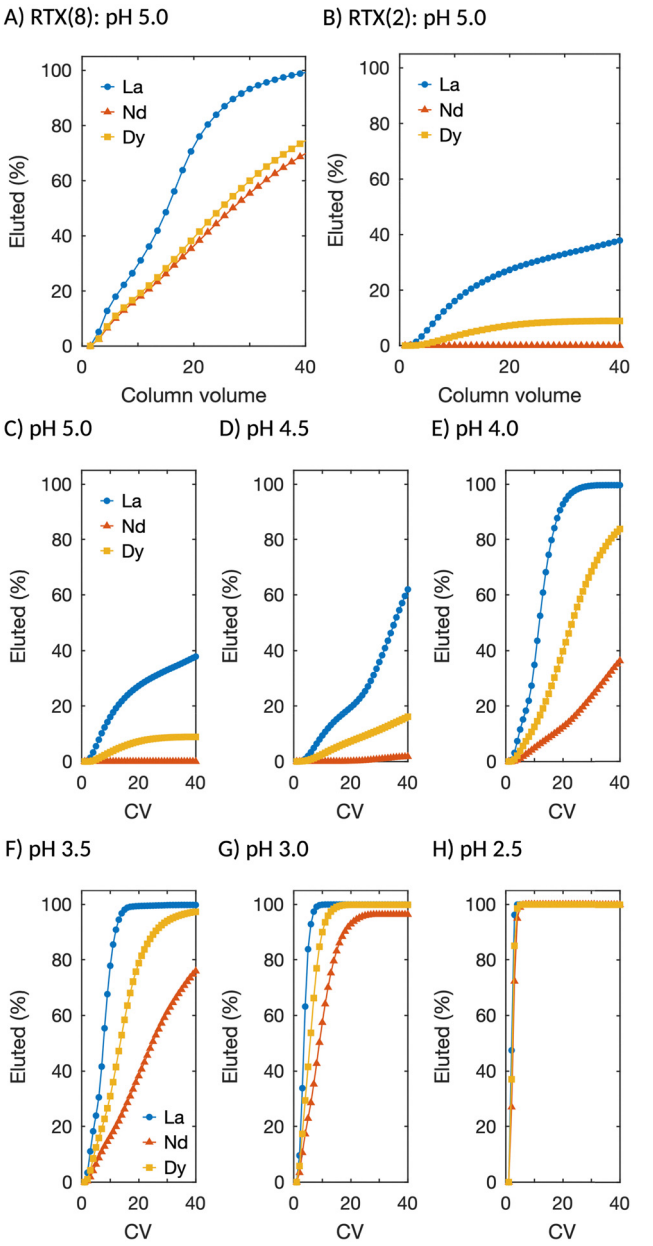

Fig. 3 Isocratic elution profiles of La, Nd, and Dy mixture using (A) RTX(8) and (B) RTX(2) illustrating significantly improved retention and selectivity at pH 5.0. (C)–(H) pH-Dependent elution behavior of RTX(2) across a range of isocratic conditions (pH 5.0 to 3.0) demonstrates the pH-tunable selectivity of RTX(2).

binding sites, which we hypothesized would enhance its separation capabilities.

Block V of the repeat-in-toxin (RTX) domain from *Bordetella pertussis* of the adenylate cyclase protein is a calcium-binding protein that functions as a molecular "ratchet," facilitating the secretion of the full RTX protein through the type I secretion system.[17] This domain, referred to hereafter as RTX(8), is intrinsically disordered in the cytosol but undergoes directional folding upon exposure to calcium-rich extracellular environments. It binds eight calcium ions sequentially from the

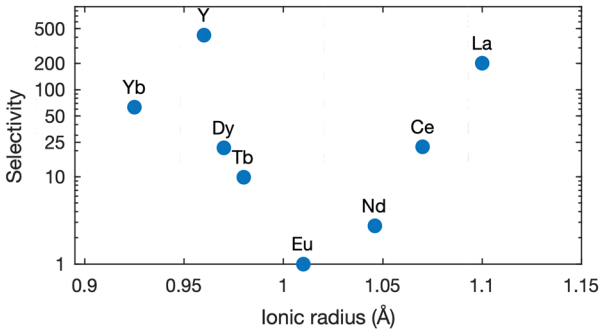

Fig. 4 Selectivity of RTX(2), referenced to Eu, demonstrates over 200-fold selectivity with the lanthanide series. Experimental details and selectivity calculations are presented in SI.

C- to N-terminus, forming a β-roll structure stabilized by a C-terminal capping group (Fig. 1A).[17–20] RTX(8) binds lanthanides with higher affinity than calcium, can strongly discriminate against non-REEs and maintains its folded conformation under highly acidic conditions (pH < 1), making it an attractive scaffold for industrial applications.[12] However, the polarized folding of the scaffold generates a cooperative binding behavior and a steep affinity gradient across the protein. This heterogeneity results in broad REE elution profiles of mixed REEs and limits the selectivity of the scaffold within the REE series (Fig. 2A).

To better understand the affinity gradient across RTX(8), a per-site analysis of binding free energy revealed a polarized distribution of calcium-binding energies, with the strongest affinities located at the C-terminal sites (Fig. 2B). While this method does not explicitly account for water coordination, a limitation especially relevant for site 1, the trend aligns with structural features observed in previous studies. The second-shell hydrogen-bonding network showed that the C-terminal sites form a highly connected hydrogen bond network supported by tightly coordinated water molecules, likely enhancing the stability and rigidity of the pocket (Fig. 1B and 2B). Guided by these observations, we designed two truncated scaffolds: RTX(4), retaining the four C-terminal calcium-binding sites (sites 1–4), and RTX(2), preserving only two sites (sites 1 and 2) (Fig. 1B). The effect of truncation on REE binding was quantified by fusing each scaffold between a Förster resonance energy transfer (FRET) pair, cyan and yellow fluorescent proteins, and measuring binding curves *via* titration with individual REEs. Fitting the FRET response to the Hill equation revealed a nearly five-fold improvement in apparent dissociation constants for RTX(2) compared to RTX(8), which was consistent across the REE series (Fig. 2C). These results confirm the presence of a steep affinity gradient in the full-length RTX(8) and identify the C-terminal region, RTX(2), as a rigid, high-affinity binding motif, stabilized by a dense second-shell hydrogen bonding network, features likely to enhance REE selectivity in chromatographic applications.

The effect of truncation on REE selectivity was examined *via* isocratic elution profiles of a three-element mixture (La, Nd, and Dy) using covalently immobilized RTX(8) and RTX(2).

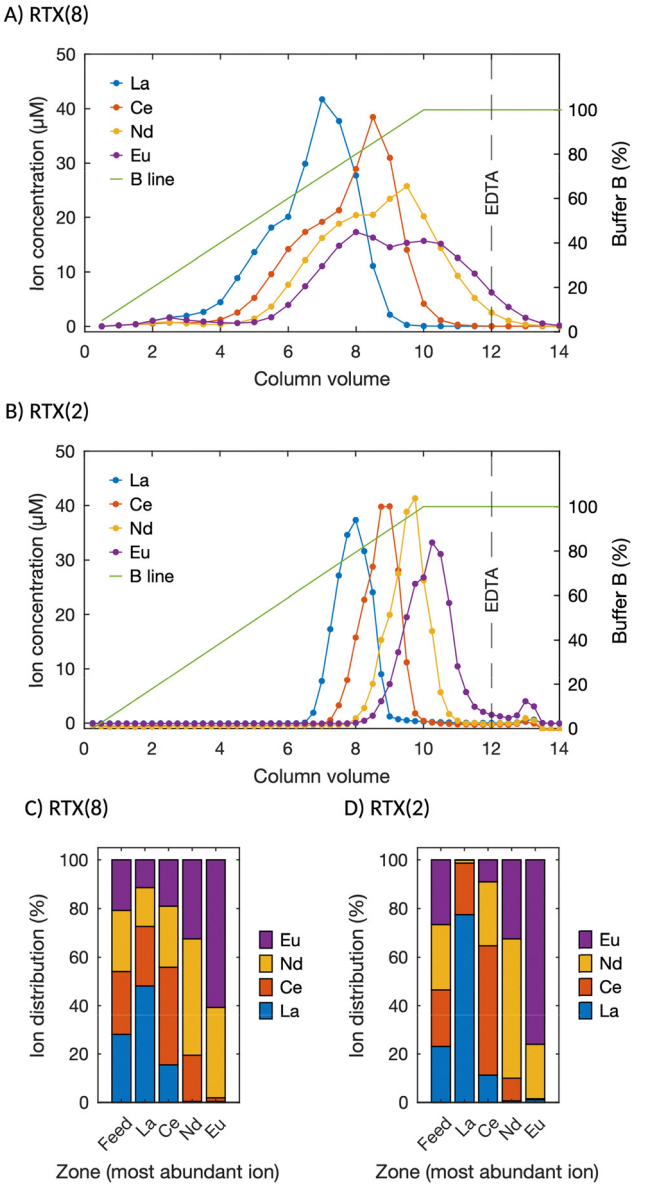

Fig. 5 (A) Elution profile of an equimolar La/Ce/Nd/Eu mixture using RTX(8) under a linear pH gradient (pH 5.0 to 3.0), showing broad peaks with limited resolution. (B) RTX(2) under the same gradient yields sharp, well-defined peaks for each REE. (C) and (D) Purity analysis of each ion based on zone fractionation, with RTX(2) showing significantly enhanced separation performance. Zones were defined based on the predominant ion in each fraction. Values are averages from triplicate runs presented in SI.

RTX(4) was not pursued for further characterization because its second-shell coordination remained more heterogeneous (Fig. 2B). RTX(8) showed weak selectivity, with all three ions co-eluting and only minor differences in retention (Fig. 3A). In contrast, RTX(2) retained ions more effectively, eluting only ~40% of La, ~10% of Dy, and virtually no Nd over 40 column volumes at pH 5.0 (Fig. 3B), indicating a substantial improvement in retention and selectivity. The scaffold was further evaluated across a range of isocratic pH conditions: over 80% of La eluted within 20 CVs at pH 4.0, Dy at pH 3.5, and Nd at pH 3.0 (Fig. 3C–H), highlighting the pH-tunable selectivity of the

Table 1 Purity and yield analysis of an equimolar La/Ce/Nd/Eu mixture separation using RTX(8) and RTX(2). The errors represent the averages of three trials

	Purity (%)		Yield (%)	
	RTX(8)	RTX(2)	RTX(8)	RTX(2)
La zone	45 ± 2	69 ± 8	92 ± 6	85 ± 4
Ce zone	40 ± 3	50 ± 5	32 ± 9	64 ± 7
Nd zone	46 ± 2	53 ± 4	23 ± 11	25 ± 6
Eu zone	60 ± 1	79 ± 3	31 ± 2	74 ± 2

scaffold. Additionally, the selectivity of the RTX(2) scaffold across the REE series was evaluated using an eight-element mixture (La, Ce, Nd, Eu, Tb, Dy, Yb, and Y), revealing over 200-fold selectivity within the series (Fig. 4).

Finally, to evaluate the separation performance of the engineered scaffold, we applied RTX(2) in the separation of an equimolar mixture of four REEs (La, Ce, Nd, and Eu) using a linear pH gradient. This was achieved by mixing buffer A (10 mM MES, pH 5.0) with buffer B (10 mM MES, pH 3.0) over a 10-column-volume elution window. RTX(8), consistent with earlier observations, produced broad and overlapping peaks with poor resolution between species and only modest enrichment of La (Fig. 5A). In contrast, RTX(2) yielded sharp, discrete elution peaks for all four REEs, with clearly improved separation profiles (Fig. 5B). To quantify separation performance, the elution curves were segmented into zones based on the most abundant ion in each fraction, and the purity and yield of each REE were calculated. RTX(2) exhibited a substantial improvement in both metrics relative to RTX(8), with certain zones showing more than a two-fold gain in recovery (Fig. 5C, D and Table 1). These results highlight the effectiveness of scaffold truncation in eliminating low-affinity sites and concentrating binding around a highly selective core, enabling finer resolution of chemically and physically similar REEs.

In summary, this study demonstrates that rational truncation of a calcium-binding RTX scaffold can significantly enhance REE selectivity by reducing site heterogeneity and concentrating binding within rigid pockets. The engineered RTX(2) variant exhibits improved binding affinity, dense second-shell hydrogen bonding, and pH-tunable resolution, enabling improved separation of REEs. These findings establish binding site homogeneity as a powerful design strategy for tuning selectivity. This approach can be broadly applicable to other metalloproteins where structural heterogeneity limits performance, promoting the development of scalable and sustainable mining.

This work was supported by DARPA's Environmental Microbes as a BioEngineering Resource (EMBER) program (FA8650-22-C-7213). The views, opinions and/or findings expressed are those of the author and should not be interpreted as representing the official views or policies of the Department of Defense or the US Government. F. K. was supported by the National Science Foundation Graduate Research Fellowship Program (NSF GRFP DGE-2036197) and the Columbia University Blavatnik Presidential Fellowship.

Conflicts of interest

A patent application (US 18/124,822) was filed covering aspects of the protein design and REE separation strategy reported in this study.

Data availability

The data supporting this article have been included as part of the SI. Experimental details and supplementary tables and figures. See DOI: https://doi.org/10.1039/d5cc03992d

References

1 E. Elbashier, A. Mussa, M. Hafiz and A. Hawari, *Hydrometallurgy*, 2021, 204.
2 V. Balaram, *Geosci. Front.*, 2019, **10**, 1285–1303.
3 Z. Chen, Z. Li, J. Chen, P. Kallem, F. Banat and H. Qiu, *J. Environ. Chem. Eng.*, 2022, **10**, 107104.
4 M. Nitz, K. J. Franz, R. L. Maglathlin and B. Imperiali, *ChemBioChem*, 2003, **4**, 272–276.
5 J. Cotruvo, E. Featherston, J. Mattocks, J. Ho and T. Laremore, *J. Am. Chem. Soc.*, 2018, **140**, 15056–15061.
6 H. Brittain, F. Richardson and R. Martin, *J. Am. Chem. Soc.*, 1976, 8255.
7 Z. Dong, J. A. Mattocks, G. J. Deblonde, D. Hu, Y. Jiao, J. A. Cotruvo and D. M. Park, *ACS Cent. Sci.*, 2021, **7**, 1798–1808.
8 J. A. Mattocks, J. J. Jung, C. Y. Lin, Z. Dong, N. H. Yennawar, E. R. Featherston, C. S. Kang-Yun, T. A. Hamilton, D. M. Park, A. K. Boal and J. A. Cotruvo, *Nature*, 2023, **618**, 87–93.
9 Z. Dong, J. A. Mattocks, J. A. Seidel, J. A. Cotruvo and D. M. Park, *Sep. Purif. Technol.*, 2024, **333**, 125919.
10 F. F. Khoury, B. S. Heater, D. R. Marzolf, S. Abeyrathna, J. W. Picking, P. Kumar, S. A. Higgins, R. Jones, A. T. Lewis, K. H. Kucharzyk and S. Banta, *Chem. Sci.*, 2025, DOI: 10.1039/D5SC02315G.
11 M. Nitz, M. Sherawat, K. J. Franz, E. Peisach, K. N. Allen and B. Imperiali, *Angew. Chem., Int. Ed.*, 2004, **43**, 3682–3685.
12 F. Khoury, Z. Su and S. Banta, *Inorg. Chem.*, 2024, **63**, 13223–13230.
13 R. Friedman, *J. Phys. Chem. B*, 2021, **125**, 2251–2257.
14 M. Wang, Q. Xiong, N. H. C. Lewis, D. Ying, G. Yan, E. Hoenig, Y. Han, O. S. Lee, G. Peng, H. Zhou, G. C. Schatz and C. Liu, *Sci. Adv.*, 2024, **10**, eadh1330.
15 E. E. Snyder, B. W. Buoscio and J. J. Falke, *Biochemistry*, 1990, **29**, 3937–3943.
16 S. S. Kt, B. Qiao, J. G. Marmorstein, Y. Wang, D. C. Favaro, K. J. Stebe, E. J. Petersson, R. Radhakrishnan, C. de la Fuente-Nunez, R. S. Tu, C. Maldarelli, M. Olvera de la Cruz and R. J. Messinger, *Chemistry*, 2025, e202501318.
17 L. Bumba, J. Masin, P. Macek, T. Wald, L. Motlova, I. Bibova, N. Klimova, L. Bednarova, V. Veverka, M. Kachala, D. I. Svergun, C. Barinka and P. Sebo, *Mol. Cell*, 2016, **62**, 47–62.
18 G. R. Szilvay, M. A. Blenner, O. Shur, D. M. Cropek and S. Banta, *Biochemistry*, 2009, **48**, 11273–11282.
19 M. Blenner, O. Shur, G. Szilvay, D. Cropek and S. Banta, *J. Mol. Biol.*, 2010, **400**, 244–256.
20 O. Shur and S. Banta, *Protein Eng., Des. Sel.*, 2013, **26**, 171–180.

